Comput Visual Sci 2: 63–68 (1999)

Computing and
Visualization in Science

Regular article

A staggered scheme for hyperbolic conservation laws applied to unsteady sheet cavitation

D.R. van der Heul[*], **C. Vuik, P. Wesseling**

J.M. Burgers Center and TU Delft, Mekelweg 4, 2628 CD Delft, The Netherlands

Received: 25 February 1999 / Accepted: 17 June 1999

Communicated by: M. Espedal and A. Quarteroni

Abstract. We demonstrate the advantages of discretizing on a staggered grid for the computation of solutions to hyperbolic systems of conservation laws arising from instationary flow of an inviscid fluid with an arbitrary equation of state. Results for a highly nonlinear, nonconvex equation of state obtained with the staggered discretisation are compared with those obtained with the Osher scheme for two different Riemann problems. The staggered approach is shown to be superior in simplicity and efficiency, without loss of accuracy. The method has been applied to simulate unsteady sheet cavitation on a NACA0012 hydrofoil. Results show good agreement with those obtained with a cavity interface tracking method.

1 Introduction

Our aim is to show the advantages of a staggered scheme for computation of solutions to hyperbolic systems of conservation laws arising from instationary flow of an inviscid fluid with an arbitrary equation of state. This contribution is an extension of the work of [1], where it has been shown how to achieve work and accuracy uniform in the Mach number M for perfect gas flow, by discretizing on a staggered grid and application of a scaling which removes the singularity for the limit of $M \downarrow 0$ in the system of equations.

The equation of state we choose has been used to model hydrodynamic cavitation in channels [5] and on hydrofoils [8] with the Euler equations. This equation of state makes the density equal to the density of vapor when the pressure drops below the vapor pressure and equal to the undisturbed liquid density above the vapor pressure, with a smooth transition between the two states. The cavitation bubble will appear in the flow domain as the region where the density is below $(1+\epsilon)\cdot\rho_{\text{vapor}}$. Contrary to methods that track the cavity interface [3, 7, 9], this method allows for free growth and even bifurcating behavior of the bubble (the shedding of a detached part of the bubble in the flow).

[*] Supported by The Netherlands Organization for Scientific Research (NWO)

The mathematical model has the following special features:

1. The speed of sound varies from low to very high values, causing the flow to be highly compressible locally, while being almost incompressible in other parts of the domain: $10^{-3} < M < 25$.
2. The nonconvexity of the equation of state makes it possible that both compression shocks and expansion shocks occur that satisfy the entropy condition. The numerical method has to select only physical weak solutions that satisfy the entropy condition.
3. For the perfect gas system of Euler equations, the flux is a homogeneous function of order one. In our case this property is lost. Many flux-splitting schemes designed for the Euler equations make explicitly use of this property, so that they cannot be applied directly to our case.
4. In the limiting case of (almost) instantaneous phase transition, the equation of state will be an (almost) discontinuous function of the pressure.

Although the flow is assumed to be isothermal, the equation of state can easily be extended with an arbitrary dependence on the enthalpy, in the same way as is done for the perfect gas case [1]. For instance in the case of cavitating flow of cryogenic fluids, the dependence of the vapor pressure on the temperature has to be taken into account.

In Sects. 2 and 3 we discuss the governing equations of the cavitation model. Section 4 contains a description of the solution algorithm employed. In Sect. 5 our approach is validated by comparison with the Osher scheme for two different Riemann problem test cases. Finally, application of the method to the simulation of unsteady sheet cavitation is discussed in Sect. 6.

2 Conservation equations

We employ the isothermal Euler equations, completed with the earlier mentioned equation of state. Although the medium in the transition between the liquid and vapor state is highly compressible, the liquid state is almost incompressible, characterized by a Mach number of order 10^{-3}. Therefore use is

made of the following Mach-uniform pressure based formulation of the compressible Euler equations [1]:

$$\frac{d\rho}{dp}\frac{\partial p}{\partial t} + (\rho U^\alpha)_{,\alpha} = 0, \tag{1}$$

$$\frac{\partial \rho U^\alpha}{\partial t} + (\rho U^\alpha U^\beta)_{,\beta} = -(g^{\alpha\beta} p)_{,\beta}. \tag{2}$$

completed with a barotropic equation of state $\rho = \rho(p)$. We use general coordinates and tensor notation, with $U^\alpha = \boldsymbol{a}^{(\alpha)} \cdot \boldsymbol{u}$ denoting the contravariant velocity components, $g^{\alpha\beta}$ the contravariant metric tensor and $\boldsymbol{a}^{(\alpha)}$ the contravariant base vector with respect to the mapping $Q : \boldsymbol{x} = \boldsymbol{x}(\boldsymbol{\xi})$, where $\boldsymbol{x}$ are Cartesian coordinates, while $\boldsymbol{\xi}$ are general boundary-fitted coordinates. For details on spatial discretisation and time integration we refer to [1].

3 Equation of state

The equation of state as treated in [6] and [11] is constructed from an empirical point of view. It is known that the density of the mixture should be the density of the liquid above the vapor pressure and it should be equal to the density of vapor well below the vapor pressure. The transition region is constructed based on empirical knowledge of the speed of sound in a bubbly mixture. As we only need the relation between pressure and density in the computational process an incomplete equation of state suffices [10].

3.1 Thermodynamic constraints

In theory one should first derive a complete equation of state $E(V, S)$, and from this an incomplete equation of state $P(V, E)$. It should be noted that the complete equation of state should respect the three laws of thermodynamics and that completing an incomplete equation of state with an entropy function to obtain a complete equation of state may not be possible nor unique. Only if an incomplete equation of state can be completed to obtain a complete equation of state, the former can be regarded as a physical constitutive relation [10]. In the isothermal case an equation of state $E(S, V)$ can be characterized by the following parameters:

– The adiabatic exponent:

$$\gamma = -\frac{V}{P}\left.\frac{\partial P}{\partial V}\right|_S, \tag{3}$$

– The fundamental derivative:

$$\mathcal{G} = -\frac{1}{2}\frac{\partial^3 E/\partial V^3\big|_S}{\partial^2 E/\partial V^2\big|_S} = \frac{1}{2}\frac{V^2}{\gamma P}\left.\frac{\partial^2 P}{\partial V^2}\right|_S, \tag{4}$$

plus the asymptotic behavior of the equation of state.
We make the following remarks:

– Thermodynamic stability requires γ to be strictly nonnegative [10]. Therefore the function $P(V)$ should be monotonically decreasing. As a result a mixture equation of state maintaining the isothermal behavior during phase transition will be thermodynamically unstable. This can be avoided by keeping a finite speed of sound in the transition region.
– Thermodynamics does not put a requirement on the sign of $\mathcal{G}$ [10]. However, if $\mathcal{G}$ changes sign within the domain, simple wave solutions will have a more complicated, so called composite, structure, which is discussed in Sect. 5. Furthermore, if $\mathcal{G}$ does not exist, discontinuous solutions will not be stable against shock splitting [10]. This means that, as opposed to the strictly convex case, a perturbation can split up a discontinuity in two separate shocks.
– Natural requirements on the asymptotic behavior of $P(V)$ are [10]:

$$\lim_{V\to 0} P(V) = \infty, \quad \lim_{P\to 0} V(P) = \infty, \tag{5}$$

since $P(V)$ is obviously invertible under the demand of thermodynamic stability.

3.2 The model equation of state

An equation of state is constructed, which has more parameters to control its behavior than the equation of state of [6] and [11]. The equation of state has the following form:

$$\begin{aligned}
&\rho = \rho_0 + c_1 p; && p < p_1\\
&\rho = \rho_0 + c_1 p + c_2 * \sum_{i=1}^{n} a_n \xi^n; && p_1 \le p \le p_2\\
&\rho = c_3 + c_4\,(p - p_2)\,; && p_2 < p
\end{aligned} \tag{6}$$

where :

$$\xi = \frac{p - p_1}{p_2 - p_1} \tag{7}$$

The following parameters can be adjusted

1. Speed of sound in the vapor state: $c_1^{-1/2}$.
2. Speed of sound in the liquid state: $c_4^{-1/2}$.
3. Transit pressures : p_1/p_2.
4. Degree of continuity C^{n-1}, by adjustment of a_n, $1 \le n \le 9$.

Altough pure water is almost incompressible, a small amount of undissolved gas, that is always present in industrial applications, can lower the speed of sound considerably.

Unlike the equation of state in [6, 11], we also treat the vapor phase as compressible, to match the thermodynamically correct asymptotic behavior of the isotherm for the limit of vanishing pressure.

Ensuring high differentiability of the equation of state across the transition region diminishes the chance of shock splitting.

4 Solution procedure

For the time-stepping procedure use is made of a nonlinear variation of an isothermal version of the compressible pressure correction method as described in [1] for the ideal gas case:
First a prediction of the momentum $(m^\alpha)^*$ is made:

$$\frac{(m^\alpha)^* - (m^\alpha)^n}{\delta t} + \left((m^\alpha)^*(U^\beta)^n\right)_{,\beta} = -(g^{\alpha\beta} p^n)_{,\beta}, \tag{8}$$

where

$$m^\alpha = \rho U^\alpha. \tag{9}$$

We are free to discretize the convection term in an upwind manner to incorporate thermodynamic irreversibility in the numerical model, whereas in the colocated case this would require some form of flux-splitting, which is not trivially extended to the case of an arbitrary nonconvex equation of state.

A momentum correction of the following form is postulated and substituted in the continuity equation:

$$\delta m = -\delta t \left(g^{\alpha\beta}\delta p\right)_{,\beta}, \tag{10}$$

$$\delta m \equiv m^{n+1} - m^*, \tag{11}$$

$$\delta p \equiv p^{n+1} - p^n. \tag{12}$$

Combination with the continuity equation leads to the following pressure correction equation:

$$\frac{\delta\rho}{\delta t} - \delta t \left(g^{\alpha\beta}\delta p\right)_{,\alpha\beta} = (m^\alpha)^*_{,\alpha}. \tag{13}$$

This solution method has computational complexity almost uniform in M [1].

4.1 Nonlinear pressure correction

In the perfect gas case the discrete linearized pressure correction equation (13) is given by the following linear system:

$$\left(\frac{d\rho}{dp}\right)^n \delta p - \delta t^2 DG\delta p = -\delta t Dm^*, \tag{14}$$

where D and G are discretizations of the divergence and gradient operators respectively. However, for our artificial medium this linearisation will no longer be a good approximation of the nonlinear system in the case of phase transition within one time step. Furthermore, $\rho'(p)$ does not exist for the case of a discontinuous equation of state modeling instantaneous phase transition.

To circumvent usage of this derivative, we have to solve the discretised version of the nonlinear system (13):

$$\rho(p^n + \delta p) - \rho(p^n) - \delta t^2 DG\delta p = -\delta t Dm^*. \tag{15}$$

Standard algorithms for nonlinear systems, e.g. Newton-Raphson, fail to work in the case of a strongly varying Jacobian.

Therefore we solve (15) with a nonlinear Gauss-Seidel algorithm where we can choose a very robust method for solving the individual nonlinear scalar equations. Application of Gauss-Seidel gives a sequence of scalar equations of the following form:

$$\rho(p^n + \delta p^{(k+1)}) - \delta t^2 A\delta p^{(k+1)} = \rho(p^n) - \delta t Dm^* - \delta t^2 B\delta p^{(k)}, \tag{16}$$

where $A - B = DG$ is a Gauss-Seidel splitting of DG. This system can be solved recursively at a price of one scalar nonlinear solve per step. The most robust way to solve a nonlinear scalar equation without using derivatives is by bisection. We choose a more efficient Dekker-type algorithm formulated by Brent [2], which also guarantees convergence if the function values in the end points of the starting interval have opposite sign, but gives superlinear convergence when the iterate closely approaches the solution.

However, the Gauss-Seidel algorithm is known to converge very slowly. To overcome this difficulty we accelerate the algorithm by using intermediate linearized steps. Every iterative step is split into a nonlinear Gauss-Seidel step followed by a linearized step which can be solved by a more efficient iterative linear solver. A more detailed description is as follows:

First, compute a nonlinear Gauss-Seidel step to obtain a first estimate $\delta p^{1/2} = p^{(k+1/2)} - p^{(k)}$:

$$\rho(p^{(k+1/2)}) - \delta t^2 A(p^{(k+1/2)} - p^n) = \rho(p^n) - \delta t Dm^* - \delta t^2 B(p^{(k)} - p^n). \tag{17}$$

Next, substitute our estimate for p^{n+1}, namely $p^{(k+1)}$, in (15) and subtract the following known term in the left and right hand side:

$$\rho(p^{(k+1/2)}) - \delta t^2 DG\, p^{(k+1/2)} \tag{18}$$

to find an equation for $\delta p^1 = p^{(k+1)} - p^{(k+1/2)}$:

$$\rho(p^{(k+1)}) - \rho(p^{(k+1/2)}) - \delta t^2 DG(p^{(k+1)} - p^{(k+1/2)}) = \rho(p^n) - \rho(p^{(k+1/2)}) - \delta t Dm^* + \delta t^2 DG(p^{(k+1/2)} - p^n). \tag{19}$$

The nonlinear term $\rho(p^{(k+1)}) - \rho(p^{(k+1/2)})$ is replaced by $\frac{d\rho}{dp}\delta p^1$. The exact derivative $\frac{d\rho}{dp}$ is replaced by an estimate $\tilde{\rho}'$ in the following secant type of way:

$$\tilde{\rho}' = \frac{\rho(p^{(k+1/2)}) - \rho(p^{(k)})}{p^{(k+1/2)} - p^{(k)}}, \qquad \left|p^{(k+1/2)} - p^{(k)}\right| \geq \mu \left|p^{(k)}\right|; \tag{20}$$

$$\tilde{\rho}' = \frac{\rho((1+\mu)p^{(k)}) - \rho(p^{(k)})}{\mu p^{(k)}}, \quad \left|p^{(k+1/2)} - p^{(k)}\right| < \mu \left|p^{(k)}\right|. \tag{21}$$

where μ is a parameter to be chosen in relation to $|p_1 - p_2|$ in the equation of state. This results in the following linear system for the second part of the pressure correction δp^1:

$$\tilde{\rho}'\delta p^1 - \delta t^2 DG\delta p^1 = \rho(p^n) - \rho(p^n + \delta p^{1/2}) + \delta t^2 DG\delta p^{1/2} - \delta t Dm^*. \tag{22}$$

This system is solved for δp^1 by preconditioned GMRES.

Finally, the total pressure correction $\delta p^{(k)} = \delta p^{1/2} + \delta p^1$ is computed and used as initial iterand for the next iteration step.

It is clear that in the case of convergence the right hand side of the system (22) vanishes and the second part of the pressure correction will tend to zero. When $\|\delta p^1\|_\infty < \epsilon$ the iteration is terminated.

If the equation of state is fairly smooth, the algorithm will not perform better than the linearized pressure correction equation, but its superiority becomes clear when p_1 and p_2 are brought closer together.

5 Remarks on validation

Weak solutions of hyperbolic systems are made unique by imposing the requirements, that shocks satisfy the jump condition (Rankine-Hugoniot), and that characteristics converge into and do not emanate from shocks (entropy condition). It is well-known that numerical schemes easily violate one or both of these conditions. Therefore convergence of the staggered scheme needs to be validated. A theory of convergence is lacking, as for many commonly used schemes. We will carry out validation by comparison with exact solutions and with another scheme. Standard finite volume schemes for the Euler equations are of colocated type and use some form of flux-splitting or approximate Riemann solution for the numerical flux at cell boundaries. For two reasons we select the Osher scheme [12] for comparison. First, it applies to general hyperbolic systems and is not restricted to the Euler equations for a perfect gas. Second, there is a proof [12] that it gives numerical solutions that satisfy the jump and entropy conditions, if shocks are sufficiently weak.

5.1 The Riemann problem for the nonconvex case

For the following two different initial states the numerical solution to the Riemann problem is compared to the exact solution:

Problem 1: $U_{\text{left}} = U_{\text{right}} = 0,\ p_{\text{left}} > p_{\text{right}}.$
Problem 2: $U_{\text{left}} < U_{\text{right}} = 0,\ p_{\text{left}} > p_{\text{right}},\ \rho U_{\text{left}} = \rho U_{\text{right}}.$

For an isothermal perfect gas, the structure of the Riemann problem always consists of two waves, namely one right running and one left running shock or expansion fan. In the case of a nonconvex equation of state either of the two waves can be composed of a number of single expansion fans and shocks, so-called compound waves. By a Lagrangian transformation the barotropic Euler equations are transformed to the p-system:

$$V_t + m_x = 0, \tag{23}$$

$$m_t + p(V)_x = 0. \tag{24}$$

For the p-system the solution of the Riemann problem is found by construction of the backward and forward wave curves, that is all states in the phase plane, that can be connected by a combination of shocks and simple waves to the left and right state [13]. The middle state, between the left and right running wave is found as the intersection of the 1-wave curve of the initial left state and the 2-backward wave curve of the initial right state. Figure 1 shows the initial states in the equation of state, the wave curves and the structure of the solution in the x/t plane for the second test case (Lagrangian frame).

The left running wave is composed of an expansion fan, an expansion shock and another expansion fan, while the right running wave is just a single compression fan. Although the fundamental derivative changes sign in the domain, the wave curves are still monotonous functions of V and therefore the solution to the Riemann-problem is unique [10].

5.2 Results

Figures 2 and 3 show results for both testcases for the staggered scheme (bottom) and the Osher scheme (top).

For both testcases the two schemes converge to the correct solution with the same accuracy in the eyeball-norm. However, due to the fact that the Osher scheme requires calculation of the eigenvectors and numerical evaluation of integral relations to obtain the Riemann-invariants, it is a few hundred times slower than the staggered scheme. To avoid evaluation of the integral relations, the Riemann invariants could be tabularized, but even then the Osher scheme would still be more costly to apply.

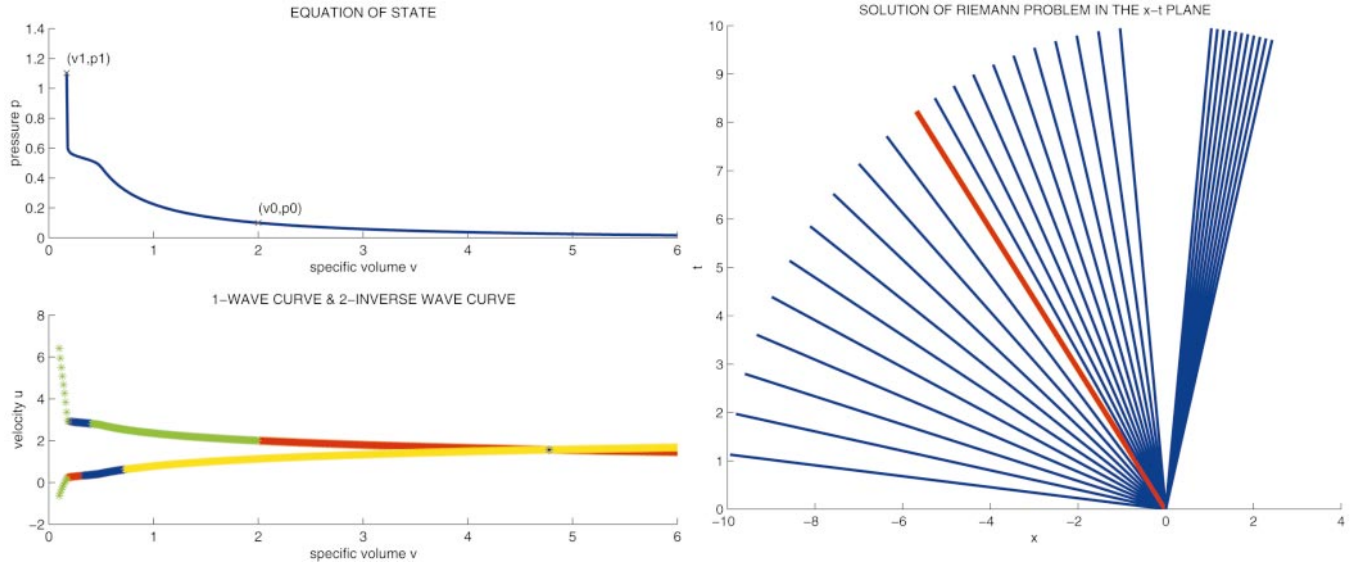

Fig. 1. Construction of the exact solution

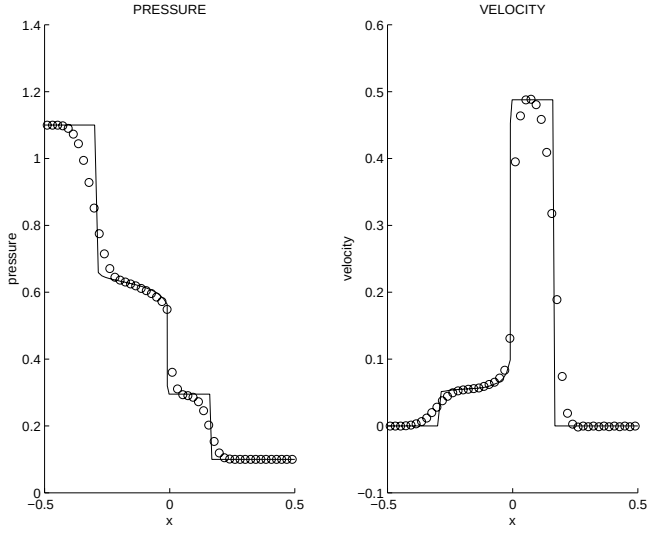

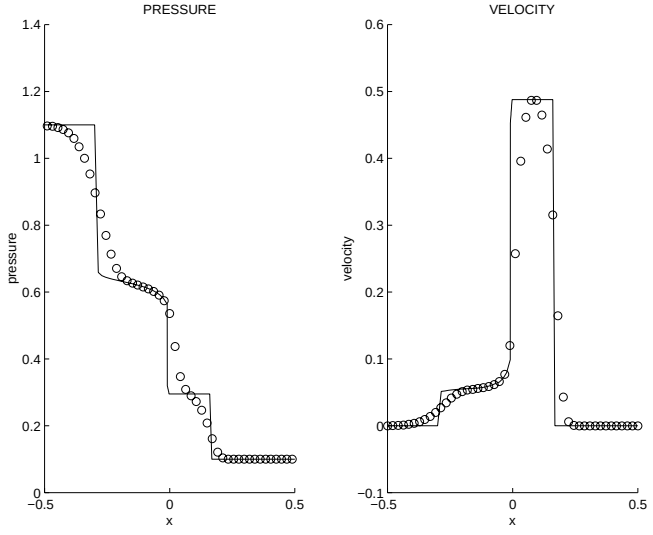

Fig. 2. Riemann problem 1; 48 cells; $\tau/h = 0.4$

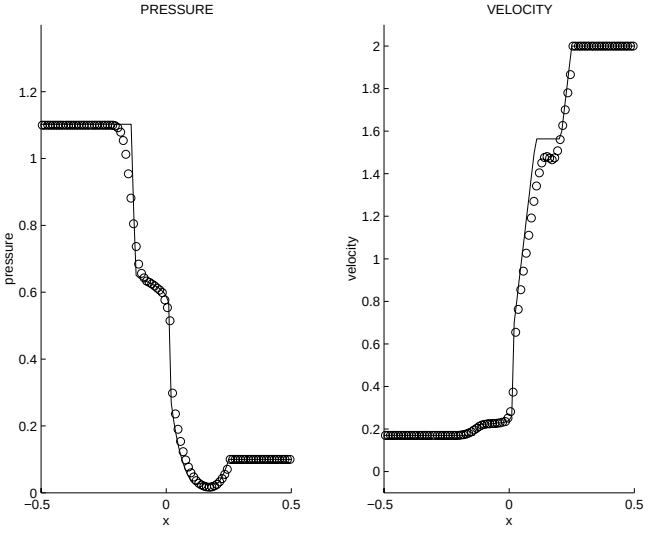

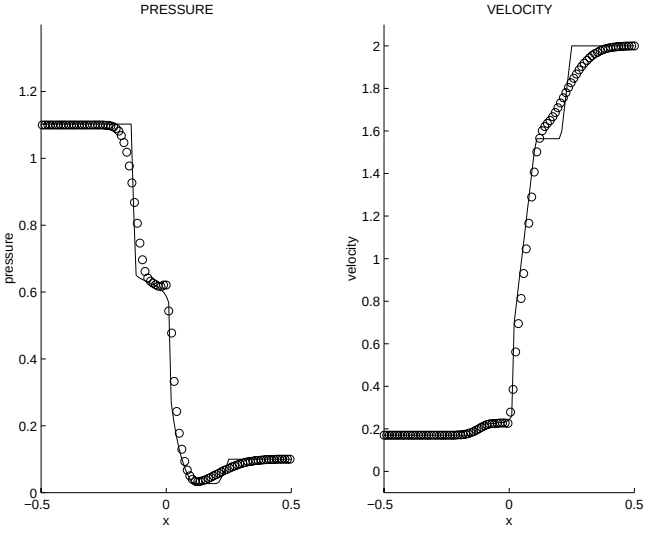

Fig. 3. Riemann problem 2; 96 cells; $\tau/h = 0.4$

Table 1. Properties of the mixture equation of state

$c_{\text{vapor state}}/c_{\text{liquid state}}$	1
$c_{\text{liquid state}}/c_{\text{minimal}}$	670
$\rho_{\text{liquid state}}/\rho_{\text{vapor state}}$	400

6 Unsteady sheet cavitation on NACA0012 hydrofoil

With the present method a simulation is made of an unsteady sheet cavity on a NACA0012 hydrofoil at 5 degrees of attack and a cavitation number $\sigma = 1.2$, where σ is defined as:

$$\sigma = \frac{p_\infty - p_{\text{vapor}}}{\frac{1}{2}\rho_\infty V_\infty^2}. \tag{25}$$

The properties of the mixture equation of state used are listed in Table 1. A C-type grid was used with 164×20 cells.

From experiments [4] it is known that the cavity shows a cyclic behavior. Initially a small bubble is formed, which will grow in time. After the cavity has attained its maximum length a re-entrant jet starts to develop at the trailing edge of the bubble. The jet will move towards the leading edge of the cavity along the hydrofoil surface. When it meets the upper part of the water/vapor interface, the aft part of the bubble is detached and convected away from the surface. When the detached bubble is sufficiently removed from the hydrofoil the cavity length will increase again. The results displayed in Fig. 4 show this behavior.

Figure 5 shows the pressure distribution on the hydrofoil just before the re-entrant jet starts to develop. Note the plateau of constant pressure underneath the cavity.

The maximum attained cavity length of 34 percent of the chord length corresponds to the results of the interface tracking method of [7]. In [7] a cavity length of 30 percent is found, but the method is reported to slightly underpredict the length in most cases.

Compared to the methods in [8] and [6] our approach is more efficient. The former uses the method of artificial compressibility, while the latter uses a modified SIMPLE approach to handle the incompressible region. Especially when

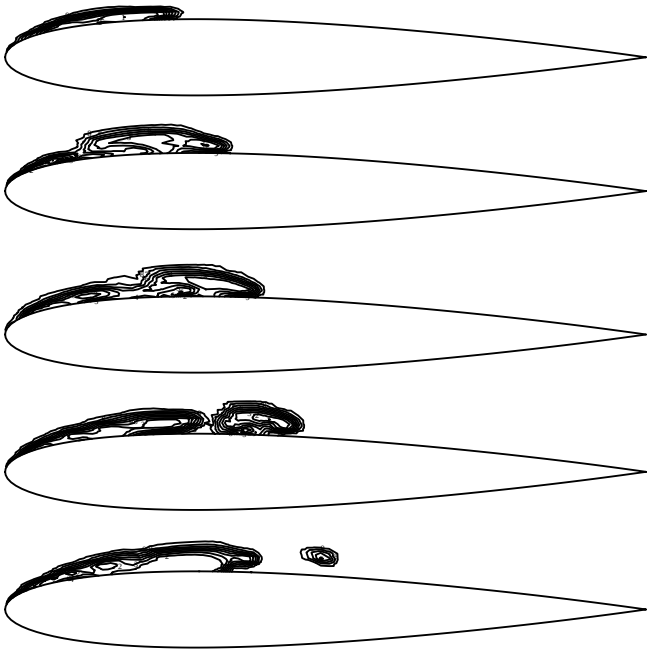

Fig. 4. Isodensity lines showing cyclic behavior of cavity

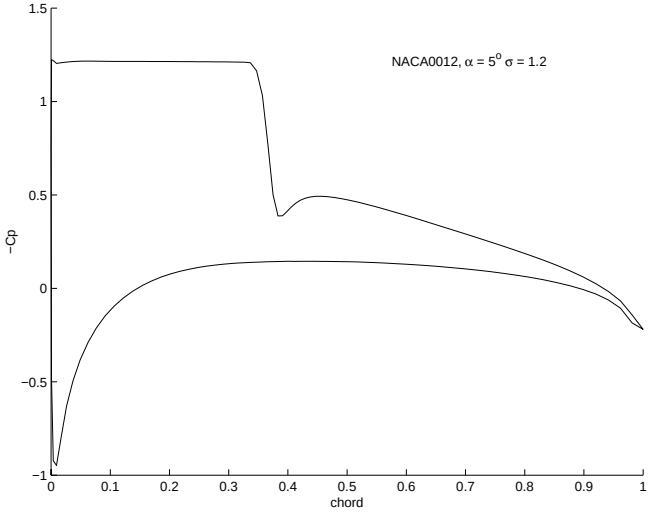

Fig. 5. Pressure distribution

the cavitation number is sufficiently small and the cavity is highly unsteady, both methods require a large number of iterations per time-step, as opposed to our single iteration per time-step solution procedure.

7 Conclusions

We have shown the simplicity and efficiency of a staggered scheme for the computation of solutions to a hyperbolic system of conservation laws arising from instationary flow of an inviscid fluid with a general equation of state. A nonlinear compressible pressure correction, based on accelerated nonlinear Gauss-Seidel, is introduced, which is more robust than a linearized formulation, in the case of a highly nonlinear or nonsmooth equation of state. The method has been applied to the calculation of unsteady sheet cavitation on a NACA0012 hydrofoil. Results agree well with those obtained with an interface capturing method.

8 Future extensions

The aim is to apply the method to the modeling of cavitation in cryogenic fluids, e.g. liquefied H_2 and O_2. Cavitation in cryogenic fluids is encountered in high performance centrifugal pumps, that are used in rocket propulsion systems. In this case the system has to be extended with a mixture enthalpy equation, because for cryogenic fluids the vapor pressure strongly depends on the temperature.

References

1. Bijl, H., Wesseling, P.: A unified method for computing incompressible and compressible flows in boundary fitted coordinates. J. Comput. Phys. 141, 153–173 (1998)
2. Brent, R.P.: Algorithms for Minimization without Derivatives. Prentice-Hall series in automatic computation. Prentice-Hall: Englewood Cliffs 1973
3. Chen, Y., Heister, S.D.: A numerical treatment for attached cavitation. J. Fluids Eng. 116, 613–618 (1994)
4. de Lange, D.F.: Observation and Modelling of Cloud Formation behind a Sheet Cavity. PhD thesis, Universiteit Twente 1996
5. Dellanoy, Y., Kueny, J.L.: Two phase flow approach in unsteady cavitation modelling. In Furuya, O., (ed). Cavitation and Multiphase Flow. FED-98, pp. 153–158. American Society of Mechanical Engineers 1990
6. Dellanoy, Y.: Modélastion d' écoulements instationnaires et cavitants. PhD thesis. INPG Grenoble 1989
7. Deshpande, M., Feng, J., Merkle, C.L.: Cavity flow predictions based on the Euler equations. J. Fluids Eng. 116(1), 36–44 (1994)
8. Janssens, M.: Calculations of unsteady attached cavitation. Master's thesis. Delft University of Technology 1996
9. Lanzenberger, K.: Numerische und Analytische Ansätze zur Simulation kavitierender Strömungen. PhD thesis. Fakultät für Machinenbau. Universität Karlsruhe 1995
10. Menikoff, R., Plohr, B.J.: The Riemann problem for fluid flow of real materials. Rev. Modern Phys. 61(1), 75–130 (1989)
11. Merkle, C.L., Feng, J.Z., Buelow, P.E.O.: Computational modelling of the dynamics of sheet cavitation. In Michel, J.M., Kato, H. (eds). Third International Symposium on Cavitation. Vol. 2, pp. 307–311 (1998)
12. Osher, S., Solomon, F.: Upwind difference schemes for hyperbolic systems of conservation laws. Math. Comp. 38, 339–374 (1982)
13. Wendroff, B.: The Riemann problem for materials with non-convex equations of state I: Isentropic flow. J. Math. Anal. Appl. 38, 454–466 (1972)